

ASE suppression in a high energy Titanium sapphire amplifier

Klaus Ertel, Chris Hooker, Steve J. Hawkes, Bryn T. Parry and John
L. Collier

Central Laser Facility, STFC Rutherford Appleton Laboratory,
Chilton, Didcot, OX11 0QX, United Kingdom

k.ertel@rl.ac.uk

<http://www.clf.rl.ac.uk/Facilities/AstraWeb/AstraGeminiHome.htm>

Abstract: The energy required to generate ultrashort pulses with petawatt peak power from a Ti:sapphire laser system is a few tens of joules. To achieve this, the final amplifier must have a gain region of around 5 cm diameter that is uniformly pumped at high fluence. The high level of amplified spontaneous emission (ASE) in such an amplifier will seriously degrade its performance unless care is taken to minimise the transverse gain and the internal reflections from the crystal edges. In developing the amplifiers for the Astra Gemini laser system, we have combined the techniques of beam homogenisation and double-pass pumping of a lightly-doped crystal with a new index-matched absorber liquid. Our results demonstrate that this combined approach successfully overcomes the problem of gain depletion by ASE in a high-energy Ti:sapphire amplifier.

© 2008 Optical Society of America

OCIS codes: (140.3280) Laser amplifiers; (140.3590) Lasers, titanium; (140.5560) Pumping; (140.7090) Ultrafast lasers

References and links

1. M. Aoyama, K. Yamakawa, Y. Akahane, J. Ma, N. Inoue, H. Ueda, and H. Kiriya, "0.85-PW, 33-fs Ti : sapphire laser," *Opt. Lett.* **28**, 1594–1596 (2003).
2. F. Plé, M. Pittman, G. Jamelot, and J. P. Chambaret, "Design and demonstration of a high-energy booster amplifier for a high-repetition rate petawatt class laser system," *Opt. Lett.* **32**, 238–240 (2007).
3. X. Liang, Y. Leng, C. Wang, C. Li, L. Lin, B. Zhao, Y. Jiang, X. Lu, M. Hu, C. Zhang, H. Lu, D. Yin, Y. Jiang, X. Lu, H. Wei, J. Zhu, R. Li, and Z. Xu, "Parasitic lasing suppression in high gain femtosecond petawatt Ti:sapphire amplifier," *Opt. Express* **15**, 15335–15341 (2007), <http://www.opticsexpress.org/abstract.cfm?URI=OPEX-15-23-15335>.
4. W. Koechner, *Solid-State Laser Engineering* (Springer, Berlin, Heidelberg, 1996).
5. M. P. Kalachnikov, V. Karpov, H. Schonnagel, and W. Sandner, "100-terawatt titanium-sapphire laser system," *Laser Physics* **12**, 368–374 (2002).
6. C. Kopp, L. Ravel, and P. Meyrueis, "Efficient beamshaper homogenizer design combining diffractive optical elements, microlens array and random phase plate," *J. Opt. A* **1**, 398–403 (1999).
7. S. A. Akhmanov, A. I. Kovrigin, M. M. Strukov, and R. V. Khokhlov, "Frequency dependence of threshold of optical breakdown in air," *Jetp Letters-USSR* **1**, 25–29 (1965).
8. J. A. Glaze, S. Guch, and J. B. Trenholme, "Parasitic suppression in large aperture Nd:glass disk laser amplifiers," *Appl. Opt.* **13**, 2808– (1974)
9. F. G. Patterson, J. Bonlie, D. Price, and B. White, "Suppression of parasitic lasing in large-aperture Ti : sapphire laser amplifiers," *Opt. Lett.* **24**, 963–965 (1999)
10. M. E. Graham, B. I. Davis, and D. V. Keller, "Immersion liquids for ruby lasers," *Appl. Opt.* **4**, 613–615 (1965).
11. F. Plé, M. Pittman, F. Canova, and G. Jamelot, "Analysis and Solutions for Parasitic Lasing in Petawatt and Multi-Petawatt Ti:sapphire Laser Systems," in *Conference on Lasers and Electro-Optics/Quantum Electronics*

1. Introduction

The current generation of high-energy titanium-sapphire (Ti:S) laser systems regularly achieve terawatt and in some cases petawatt peak powers, output energies of several tens of Joules and focused intensities greater than $10^{20} \text{ W cm}^{-2}$ [1–3]. The pump lasers for such systems are generally frequency-doubled Q-switched YAG or YLF lasers with additional glass amplifiers, and are themselves complex and expensive laser systems. Making the most effective use of the costly pump radiation is a matter of economic good sense, but there are difficulties associated with this which require careful design to overcome. In developing the Ti:S amplifiers for the Astra Gemini laser system at the Central Laser Facility, we have used a novel approach to some aspects of pumping the crystals and the suppression of amplified spontaneous emission (ASE), which we present in this paper.

1.1. *The Astra Gemini laser system*

Astra Gemini is a petawatt-class Ti:S laser system at the Central Laser Facility at the Rutherford Appleton Laboratory in the U.K. When fully commissioned the system will deliver two beams to the customised experimental area, each with an energy of 15 J in a compressed pulse of 30 fs duration. The dual-beam design of Gemini will allow experiments to be conducted in many different geometries, with the capability of varying the focal length, relative timing and polarisation of the two beams in a variety of ways. Astra Gemini consists of two Ti:S amplifiers, each pumped by a total of 60 J of green light in two beams from a frequency-doubled Nd:glass laser system. The input to the amplifiers is the beam from the Astra system, consisting of 1.5 J of infra-red (IR) light at 800 nm in a 1 ns chirped pulse, which is split as it enters the Gemini laser area. In each of the Gemini amplifiers, the 800 nm beam makes four passes of the Ti:S crystal, and is amplified from 750 mJ to 25 J. Beam quality is maintained by image-relaying from Astra, and within the amplifiers by spatial filters between the passes. After expansion from 50 mm to 150 mm diameter, the pulses are compressed to 30 fs with an efficiency of around 70%, and then transported to the experimental area on the ground floor below the laser. The design of Gemini provides for the use of long focal length focusing optics, variable pulse duration (by detuning the compressor lengths), energy control (by varying both the pump energy and the input to the amplifiers), and the introduction of additional beams at a later date.

2. Transverse gain in a strongly pumped crystal

Large-aperture Ti:S crystals for high-power amplifiers are available in diameters up to about 12 cm. The characteristics of the crystal growth process tend to produce a variation of Ti^{3+} dopant concentration along the axis of the crystal, so to avoid excessive variations in absorption the thickness of the crystal is usually limited to a few centimetres. Typically, the crystal is pumped through its two faces with two or more beams, and the 800 nm beam to be amplified traverses the crystal in a similar direction, as shown in Fig. 1. Both the pump and the 800 nm extracting beams are vertically polarised. In this geometry the absorbed energy per unit volume is greatest at the surfaces, and falls off exponentially towards the interior. As high-energy amplifiers are made larger in the quest for greater output energy, so the diameter of the pumped region and the transverse gain-length product at the surfaces increase, to the point where gain depletion caused by ASE can severely limit the energy extracted from the amplifier. This can be assessed quantitatively in the following way. We assume a four-level system and neglect fluorescence

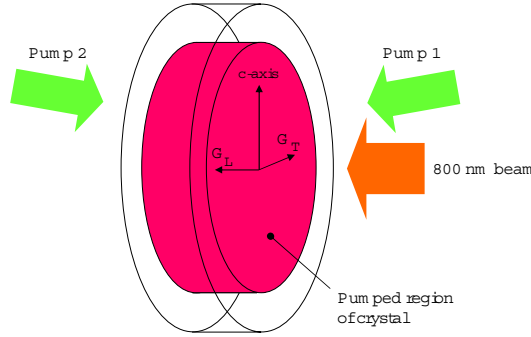


Fig. 1. Geometry of a high-power large-aperture Ti:sapphire amplifier.

decay. Pump and extraction beams propagate collinearly parallel to the optical axis in the z -direction. The small signal gain coefficient g_o can be expressed as

$$g_o(z) = E_{st}(z) \frac{\sigma_E}{h\nu_{las}} = \frac{E_{st}(z)}{F_{sat}}. \quad (1)$$

where E_{st} is the stored energy per unit volume, σ_E is the stimulated emission cross section, ν_{las} is the laser frequency and F_{sat} is the saturation fluence [4]. The z -dependence of g_o results from the fact that the pump radiation gets attenuated as it propagates through the crystal. As E_{st} does not vary perpendicularly to z we can express it as

$$E_{st}(z) = \frac{1}{A} \frac{dE_{st}}{dz}, \quad (2)$$

where A is the area of the pumped region. Considering that E_{st} results from absorbed pump radiation and that pump absorption is described by the Lambert-Beer law, we can transform Eq. (2), taking into account the quantum defect and neglecting other loss mechanisms:

$$E_{st}(z) = \frac{1}{A} \frac{\nu_{las}}{\nu_p} \frac{dE_p}{dz} = \frac{1}{A} \frac{\nu_{las}}{\nu_p} E_p(z) \alpha = \frac{\nu_{las}}{\nu_p} F_p(z) \alpha, \quad (3)$$

where ν_p is the frequency of the pump radiation, E_p is the pump energy, α is the pump absorption coefficient and F_p is the pump fluence.

Combining Eq. (1) and Eq. (3) we can now obtain an expression for the transverse gain G_T which is the gain that is experienced by a photon travelling the entire diameter D of the gain region, perpendicular to z :

$$G_T(z) = \exp\left(\frac{F_p(z)}{F_{sat}} \frac{\nu_{las}}{\nu_p} \alpha D\right). \quad (4)$$

The gain is polarisation dependent, and is greatest for light polarised parallel to the c -axis of the Ti:S crystal. Therefore G_T is greatest in the direction perpendicular to the c -axis, as shown in Fig. 1.

The longitudinal gain G_L , the gain for photons traversing the crystal parallel to the optical axis, can be calculated by integrating E_{st} along z , over the length l of the laser crystal. We then obtain

$$G_L = \exp\left(\frac{1}{F_{sat}} \int_0^l E_{st}(z) dx\right) = \exp\left(\frac{F_{st}}{F_{sat}}\right) = \exp\left(\frac{F_{abs}}{F_{sat}} \frac{\nu_{las}}{\nu_p}\right), \quad (5)$$

where F_{abs} is the absorbed pump fluence, meaning input minus output fluence. If almost all the pump radiation is absorbed, i.e. $F_{abs} \approx F_o$, where F_o is the incident pump fluence, Eq. (5)

takes on a form that does not depend on α or l . To find the relationship between G_T and G_L we consider G_T directly at the surface of the laser crystal where $F_p(z)$ is equal to the un-attenuated pump fluence F_o and hence G_T is biggest:

$$G_T(z=0) = \exp\left(\frac{F_o}{F_{Sat}} \frac{v_p}{v_{las}} \alpha D\right) \approx G_L \exp(\alpha D). \quad (6)$$

Hence, the longitudinal gain does not depend on α or D , provided the pump radiation is fully absorbed. The transverse gain at the surface however grows exponentially with these two parameters. Minimising G_T and the losses caused by transverse ASE therefore requires a laser crystal with low α and hence low doping density. Efficient use of the pump light, on the other hand, requires high absorption, which with low doping can be achieved only by a long absorption length. Despite not appearing explicitly in any of the equations above, the length of the crystal therefore plays a crucial role in minimising G_T . The obvious choices for obtaining high pump absorption at low doping are to use a long crystal or several short crystals in series, but this would result in high costs and a large amount of material in the optical path, which is undesirable for several reasons. An attractive alternative approach is a thin, low-doped crystal and pump light recycling, a scheme in which the un-absorbed pump light is collected and reflected back into the crystal for a second pass, thus doubling the effective pump absorption length.

To illustrate the benefits of pump light recycling (or double-pass pumping) we calculated $G_T(z)$ for two examples with a simple one-dimensional model. In this model first the absorbed pump energy was calculated iteratively taking into account the depletion of the ground state, then the gain coefficient was calculated as in Eq. (1). Parameters used were similar to those planned for the Astra Gemini system. In each case a 25 mm thick Ti:S crystal is pumped from both sides with beams of 50 mm diameter and pulse energies of 30 J per beam at a wavelength of 527 nm. The first case is that of a highly doped crystal that absorbs 99 % of the pump light in a single pass ($\alpha = 1.84 \text{ cm}^{-1}$), whereas in the second case the doping is such that 99 % of the light is absorbed in two passes ($\alpha = 0.92 \text{ cm}^{-1}$, with only 90 % of the light being absorbed in the first pass). The signal wavelength used for the calculation is 800 nm and the gain saturation fluence is 1 J cm^{-2} .

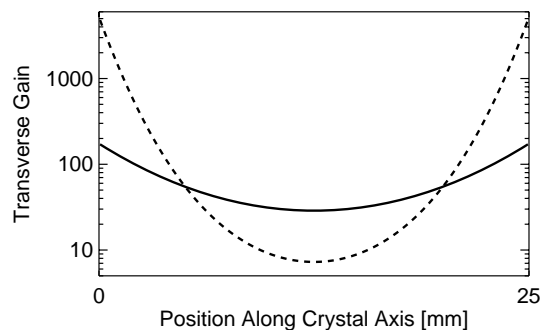


Fig. 2. Calculated transverse gain as a function of position along the optical axis of the laser crystal. Dashed line: highly doped crystal with single pass pumping; solid line: lightly doped crystal with double pass pumping.

The transverse gains as a function of position along the optical axis were calculated for these two cases and are shown in Fig. 2. In the highly doped, single-pass pumped crystal much of the gain is concentrated at the crystal faces, with the transverse gain reaching a maximum value of 4800. In the lightly-doped crystal with double-pass pumping, the gain distribution is more even and the maximum transverse gain is only 170.

3. Pump beam homogenisation

Large aperture Ti:S amplifiers require a homogeneous, flat-topped distribution of the pump light, which is very difficult to achieve by using the direct output beam of a high energy, large-aperture Nd:Glass laser system operated at a high repetition rate. The technique of beam homogenisation provides a solution to this problem. Several approaches have been described, among them segmented mirrors [5], micro lens arrays and diffractive optical elements [6]. The working principle of all these methods is to divide the incident beam into many sub-apertures which are all expanded onto the same area in the so-called target plane which lies inside the laser crystal. The resulting distribution in the target plane is ideally a homogeneous top-hat profile with steep edges. Figure 3 illustrates that principle and also shows how such a scheme can be adapted for double-pass pumping.

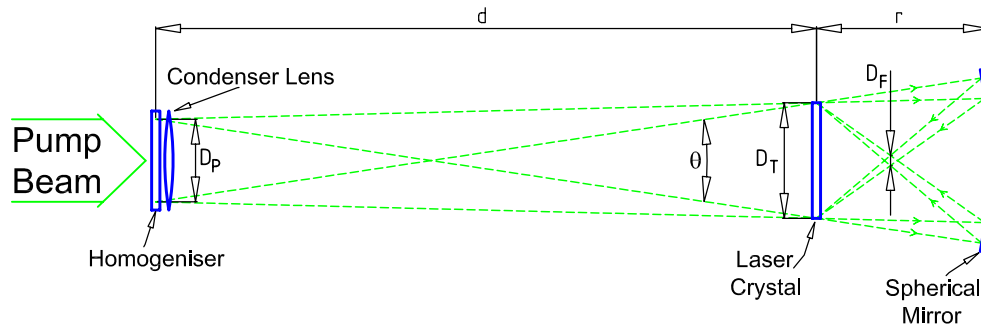


Fig. 3. Illustration of pump beam homogenisation and recycling.

The pump beam with a diameter D_P enters the beam homogeniser from the left, which is immediately followed by a condenser lens. This optic is positioned at a working distance d from the laser crystal. In the target plane, the light bundle has the diameter D_T . To visualise the extent of the light bundle before and after the laser crystal, rays from opposite edges of the homogeniser are shown. After the crystal the light bundle diverges with a full angle $\theta \approx D_P/d$. The transmitted pump is collected by a concave mirror, positioned to re-image the crystal plane onto itself. This ensures that the back-reflected distribution has the same diameter and also the same high degree of homogeneity as the original distribution. The highest intensity in this arrangement is found between the focusing mirror and the laser crystal where an image of the homogenisation optic is formed. To evaluate whether air breakdown is a concern at this location, the diameter D_F of this image can be calculated using geometrical optics. One obtains

$$D_F = D_P \left(\frac{2d}{r} + 1 \right)^{-1}. \quad (7)$$

3.1. Implementation of homogenisation and double pass pumping

To implement the scheme illustrated in Fig. 3 on Astra Gemini, we have selected diffractive optical elements (DOE) for beam homogenisation, primarily because they were readily available in the required size and could be tailored to our requirements. The DOEs were manufactured by Silios Technologies. Eight phase levels were engraved into 1 mm thick fused silica substrates by means of a plasma etching process. The devices produce multiple diffracted orders, but the phase structure is optimised to maximise the amount of light in one of the first-order beams, which is used for pumping the TiS crystal. The clear aperture of the DOEs is 65 mm and they are anti-reflection coated for 527 nm. They were specified so that $D_T = 50$ mm and $d = 4.7$ m.

Although not shown in Fig. 3, the diffracted light is directed slightly downward such that the pump spot is centred 60 mm below the optical axis. This off-axis geometry allows us to block the small portion of light in the zero order, which would otherwise be focused in the target plane by the condenser lens, and could potentially cause damage.

The optomechanical set-up of the pump beam path in Astra Gemini is implemented as follows. Each of the two Ti:S amplifiers is pumped by a frequency doubled Nd:Glass laser system (Quantel SA, France), each providing two beams with a diameter of 45 mm. The two beams are slightly expanded to 50 mm in a vacuum relay telescope. Each pump beam then passes through the beam homogenisation optics. The pump beams are folded to accommodate the long path length of 4.7 m between homogeniser and Ti:S crystal. This is possible as the beam diameter stays confined until reaching the target plane and only becomes more divergent afterwards (see Fig. 3). The long working distance was chosen in order to minimise the divergence of the pump beams after passing the laser crystal, which facilitates pump recycling, as described in the previous section. The initial pump beam paths lie in a horizontal plane above the centre of the laser crystal. The diffracted beams are deflected slightly downwards by the homogenisation optics, and the last folding mirror in each arm steers them downwards at a steeper angle so that they intersect in the centre of the laser crystal. The 800 nm beams propagate in a horizontal plane level with the centre of the laser crystal. The transmitted pump light is collected by the concave pump recycling mirrors, which are positioned beneath the 800 nm beam plane at a distance of 1.5 m from the crystal, equal to their radius of curvature.

With a maximum pump energy of 30 J in one beam, a pump pulse duration of 30 ns, a first-pass pump light absorption of 90 %, and an image spot size of 6.9 mm (see Eq. (7)), the intensity inside this image spot is $2.7 \times 10^8 \text{ W cm}^{-2}$, safely below the air breakdown threshold of $4 \times 10^{10} \text{ W cm}^{-2}$ [7]. As the DOE is a phase plate and not a micro lens array, there are no points in the system anywhere between the DOE and the crystal where small images or foci are formed.

3.2. Results of homogenisation and double pass pumping

Figure 4 shows the measured intensity distribution of one pump beam. The image was recorded with a CCD camera that images the light leaking through a high reflective laser mirror and then falling on to a diffuser screen. Figure 5 shows the light distribution that is generated in the plane of the Ti:S crystal by one pump beam after passing the homogenisation optic. This image was recorded by placing a white alumina tile in the crystal plane and imaging it with a CCD camera. Both measurements were recorded with a single pulse at an energy of 26 J while the pump laser was running at a repetition rate of 1 shot every 20 s. The raw beam profile shown in Fig. 4 is clearly not suitable for directly pumping the Ti:S amplifier. The nominal beam diameter of 45 mm is denoted by the outermost diffraction rings, but most of the energy is concentrated in a much smaller area. Inside this area, the intensity could induce optical damage, while the outer region would be only weakly pumped. We have also found that this fill factor changes as the output energy of the pump lasers is varied.

With the homogenisation optics in place, however, a near-perfect top-hat-like intensity distribution is generated in the target plane, as shown in Fig. 5. In the plateau region of the distribution (90 % of the FWHM diameter), the relative RMS intensity modulations are 6 % and the peak-to-valley modulations are 36 %. These modulations are on a fine spatial scale and their effect is largely averaged out, firstly because two pump beams and two (inverted) back-reflected beams overlap inside the laser crystal and secondly because the 800 nm beam to be amplified traverses the crystal four times at different off-axis angles.

We have so far characterised only two of our five beam homogenisers, which showed very similar results in terms of achieved homogeneity. The diffraction efficiencies into the first order beam were much greater than expected, being 93 % for one and > 95 % for the other, compared

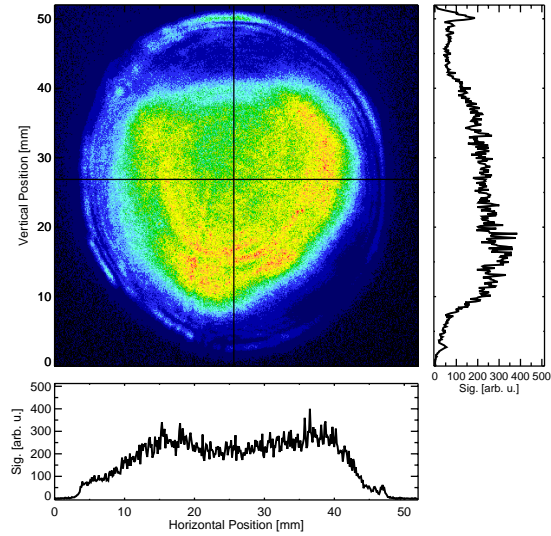


Fig. 4. Intensity distribution of raw pump beam.

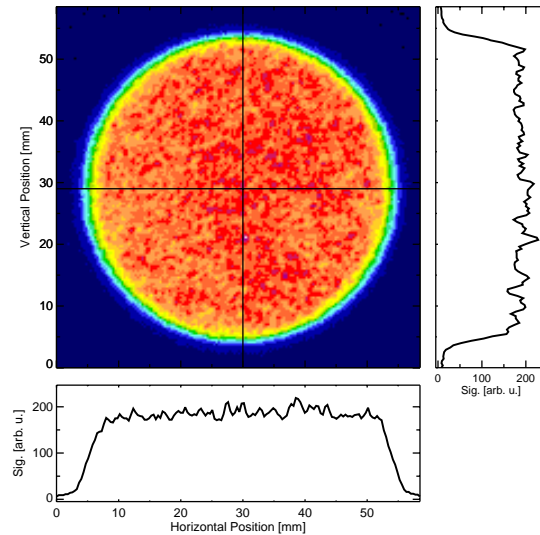


Fig. 5. Intensity distribution of homogenised pump beam in plane of Ti:S crystal.

with the 75% guaranteed by the supplier. This can be partly attributed to the small off-axis angle that results from the long working distance. Approximately 1% of the energy goes into the zero order, and the remaining few percent are distributed between the other diffracted orders.

4. Index-matched absorber

As shown in the preceding section, the use of pump recycling combined with crystals of lower absorption can greatly reduce the transverse gain-length product. However, it is equally important to prevent single-pass transverse ASE returning to the gain region from the edge of the crystal. This optical feedback can be minimised by absorbing the ASE in a suitable material,

by allowing it to leave the crystal and absorbing it elsewhere, or by a combination of these methods. The use of index-matched absorbing cladding materials to reduce parasitic lasing and ASE losses is a well-developed technique in Nd:glass lasers, and effectively combines both approaches [8]. The refractive index of sapphire, however, is 1.76 at the laser wavelength, and this greatly restricts the choice of suitable materials. There is also the potential difficulty of bonding the chosen material to the sapphire closely enough to couple the light into the cladding. One method that has been used successfully is to apply a layer of index-matched thermoplastic polymer to the cylindrical surface [9]. The polymer is doped with a material that absorbs the transverse radiation. A liquid of high refractive index in contact with the crystal would be a good choice, especially if it could be made absorbing at the laser wavelength. The refractive index of the liquid does not need to be perfectly matched to sapphire unless the cylinder surface is polished. The cylindrical edges of our crystals are fine-ground, so the feedback would come from diffuse scattering, although the high refractive index of sapphire makes this scattering stronger than it would be from glass. Another advantage of using a liquid is that it could be circulated to cool the crystal in amplifiers where the average pump power is high.

An ideal liquid for this purpose would (1) be a perfect index-match for sapphire; (2) have low toxicity; (3) not react chemically with engineering materials used for the containing cell; (4) readily dissolve an absorber for the laser wavelength (or be an absorber itself); (5) be cheap and easily available. Not surprisingly, no liquid exists that possesses all these properties.

4.1. Choice of index-matching liquid

Possibly the best-known index-matching liquid for sapphire is diiodomethane, CH_2I_2 , which has a refractive index of 1.737, and is cheap and readily available. It has the disadvantages that it is both corrosive and a severe irritant, and decomposes (slowly) when in contact with commonly-used materials such as aluminium, steel and copper alloys. A literature search uncovered one very thorough study of liquids for use with ruby lasers [10], in which more than 40 organic liquids and aqueous solutions were evaluated for their suitability as immersion media for ruby crystals. Two promising possibilities tested in the paper were (1) 1-bromonaphthalene (BN) and (2) solutions of tin(II) chloride in glycerol (TCG). BN has a refractive index of 1.66, and the authors of [10] state that TCG can be prepared as a clear colourless liquid with a refractive index up to 1.75, although no method is given.

TCG appeared attractive because the index-match is very good, the components are readily available, and its toxicity is low. We prepared a number of TCG solutions containing different concentrations of the salt. More than 20 grams of the crystalline solid could be dissolved in 2cm^3 of glycerol with ultrasonic agitation, giving a pale green solution that contained a fine precipitate. The precipitate was settled by centrifugation, and the refractive index of the resulting clear liquid was measured with an Abbe refractometer. The highest refractive index obtained was 1.69 with the most concentrated solutions, and these invariably crystallised, turning almost completely solid after a day or two. We also discovered that the solution reacted vigorously with aluminium alloys. The small increase in index over BN did not justify the effort required to prepare the large quantities of the centrifuged solution needed (around 400cm^3), so we decided to consider alternatives.

The first material suggested by [10], BN, is classified as an irritant, but it is not corrosive or as harmful as diiodomethane, and it is also cheap and easily available. Our tests showed it to be compatible with steel, copper, brass, aluminium, and silicone rubber, but not butyl rubber (commonly used for o-rings). BN also readily dissolves the laser dye IR140, which absorbs at 800 nm. We concluded that BN would be a suitable choice for our index-matching liquid, with IR140 dissolved in it as an absorber.

A stock solution of IR140 in BN containing $1\text{mg}/\text{cm}^3$ was almost opaque to visible light, so

this solution was diluted to different concentrations to make absorption measurements with a spectrophotometer. The intention was to use a low concentration of dye in order to ensure bulk absorption of the ASE, rather than allowing all the light to be absorbed in an extremely thin layer of the liquid. Table 1 shows results from these tests.

Table 1. Absorption measurements of IR140 laser dye in 1-bromonaphthalene.

| Concentration of IR140 ($\mu\text{g}/\text{cm}^{-3}$) | Absorption coefficient at 800 nm (cm^{-1}) |
|---|---|
| 10 | 0.89 |
| 20 | 1.92 |
| 30 | 2.77 |
| 40 | 3.30 |

In the mounting cell for the Ti:S crystal, described below, the liquid will be held in a 2 cm wide annulus around the crystal, so the path length to the inside of the cell and back to the crystal is 4 cm. With an absorption coefficient of 2.7 cm^{-1} , the transmission of this path would be 1.5×10^{-5} , not allowing for additional absorption and scattering at the wall of the cell. This is about 2% of the Fresnel reflection from the crystal-liquid interface and is therefore negligible.

4.2. Design of Ti:S mounting cell

The Ti:S crystal must be held in a cell with the BN around it, so the liquid is in contact with the cylindrical surface. It is also important that the crystal can be rotated around the cylinder axis, so the c-axis of the sapphire, which lies in the plane of the flat faces, can be made parallel to the polarisation of the 800 nm beam. If this is not done accurately, the birefringence of the crystal produces modulations in the spectrum which reduce the compressibility of the laser pulse. Our design for the crystal cell has a goniometer-type base which allows the crystal to

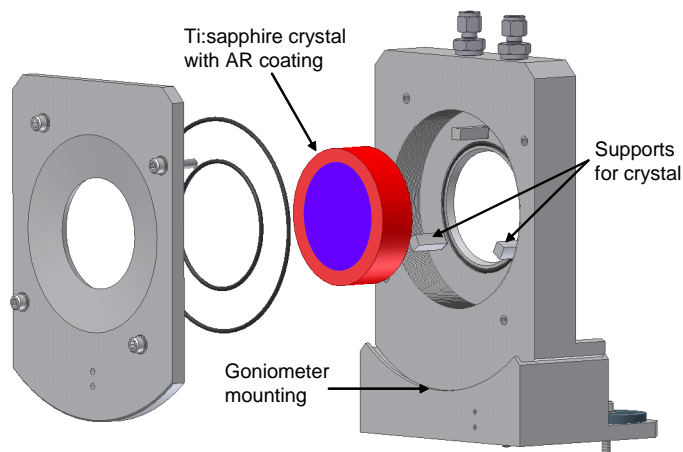


Fig. 6. Exploded view of the Ti:sapphire crystal cell and mounting.

be rotated around the cylinder axis and then locked in position. The crystals bought for the Astra Gemini project were specified with a small flat facet on the cylinder surface, such that the facet is perpendicular the c-axis within 2 degrees. This allows the crystal to be orientated fairly accurately when it is installed, so the final adjustment is small. The cell is made in two parts, and the crystal is supported on bars that are part of the larger section. Figure 6 shows an exploded view of the cell. The inner O-rings seal directly onto the flat faces of the crystal

outside the area that is anti-reflection coated. Ports for filling and emptying the cell are at the top of the assembly.

4.3. Fluorescence and gain measurements

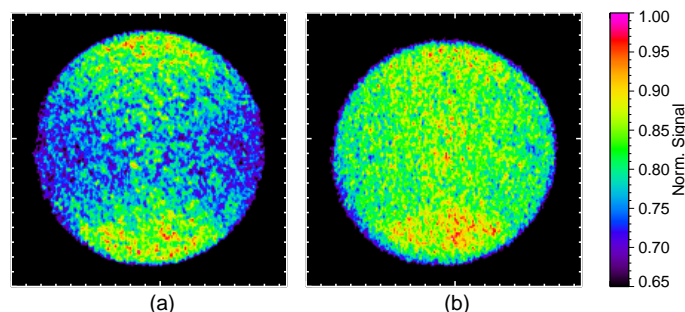


Fig. 7. Image of fluorescence of Ti:S crystal at 52 J pump energy; (a) without and (b) with index-matched absorber liquid. Images are normalised to maximum signal, signal values below 65 % of maximum are shown in black.

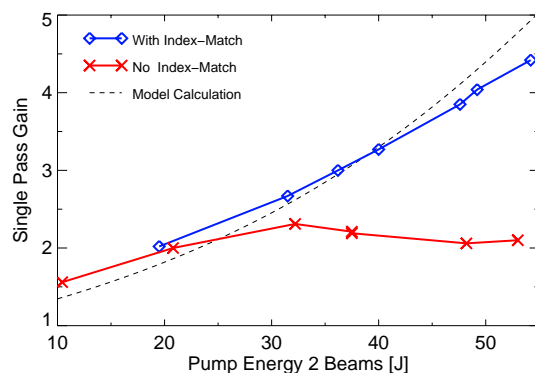


Fig. 8. Single-Pass small-signal gain with and without crystal being immersed in index-matching absorber fluid, measured as function of pump energy.

Figure 7 shows images of the fluorescence of the Ti:S crystal pumped by 52J of green light, with no 800 nm beam present. Image 7(a) was recorded with the "dry" crystal, whereas for image 7(b) the crystal was immersed in the absorber liquid. The images were recorded with a CCD camera looking at one flat input face of the crystal at near-normal angle. An RG615 filter was used to suppress stray pump light and the exposure was started a few μs before the pump pulse and stopped 34 μs later, by which time the fluorescence has completely decayed.

The most prominent difference between the two images is the appearance of an hour-glass shaped darker region along the horizontal axis in the absence of the absorber liquid. This is where the highest transverse gain occurs since the gain is polarisation-dependent and is highest for light polarised along the c-axis (see Fig. 1). Therefore, the darker region is the signature of parasitic transverse lasing. A similar signature observed by Plé et al. [11], was even more clearly defined than in our case, probably because a crystal with a polished cylindrical surface was used. We also observed a greatly reduced overall fluorescence signal for the dry crystal, compared to the crystal being immersed in the absorber liquid. Because of the normalised representation, this difference is masked in Fig. 7.

For a quantitative assessment of the effect of the index matched absorber liquid we measured the small signal gain as a function of pump energy, first with the crystal dry and then with it immersed in the liquid. The result is shown in Fig. 8. For this measurement, the 4-pass amplifier was seeded with a pulse energy of 6 mJ at 800 nm. Input and amplified pulse energies were measured with a pyroelectric energy meter (QE50, Gentec). The maximum output was 2.4 J after four passes. This output was less than 5 % of the total pump energy, so the amplifier is clearly in the small-signal regime far from saturation, and the single-pass small-signal gain is equal to the fourth root of the total gain. Without the absorber liquid, the gain increases slowly up to about 30 J of pump energy. From this point the gain appears clamped, indeed further increase in pump energy leads to the gain dropping slightly. The highest gain value obtained lies far below what is required for efficient energy extraction, and is reached too early at around 60 % of the maximum possible pump energy. This is an effective demonstration that ASE backscattering at the fine-ground crystal surface is sufficient to cause severe gain depletion. It is clearly imperative to eliminate the scattering in order to extract energy from the crystal efficiently and achieve high pulse energies. With the absorber liquid in use however, no gain clamping is observed. The gain curve starts to diverge from the one with no liquid at around 20 J of pump energy, and follows the model curve reasonably well. The gain continues to increase up to the maximum pump energy used, and shows no sign of levelling off. However, the fluorescence image in Fig. 7 does show a hint of the hourglass shape that is the signature of gain depletion by ASE, which suggests that the residual scattering at the crystal surface due to the imperfect index-match is having a slight effect. The integrated fluorescence signal from images similar to those in Fig. 7 shows near-identical behaviour to the small-signal gain curves of Fig. 8 with the absorber absent and present.

5. Conclusion

We have successfully combined techniques for efficiently pumping a large aperture high-energy Ti:S amplifier with the use of beam homogenisation and an index-matched absorber to suppress parasitic lasing. The double-pass pumping scheme we have developed allows the use of a thin, low-doped laser crystal while achieving a high level of pump light absorption. This in itself greatly reduced the transverse gain and the losses caused by ASE. We have implemented an efficient beam homogenisation scheme using diffractive optical elements that produces a uniform flat-topped energy distribution at the Ti:S crystal, and have demonstrated that beam homogenisation by this method is compatible with double-pass pumping. Immersing the cylinder face of the crystal in 1-bromonaphthalene with dissolved IR140 laser dye has proved to be highly effective at minimising gain losses due to transverse parasitic lasing, while avoiding the drawbacks of other commonly-used materials. The combination of these techniques has enabled the Astra Gemini amplifiers to reach their specified output energy, with the potential for increased output in the future.

Acknowledgments

We would like to acknowledge the contribution of Steve Hancock who designed the mounting cell for the Ti:S crystal. We would also like to thank Stéphane Tisserand of Silios Technologies for very helpful discussions.